Research Square

Preprints are preliminary reports that have not undergone peer review.
They should not be considered conclusive, used to inform clinical practice,
or referenced by the media as validated information.

Study of High-Performance Protective Coatings of Bio-Based UV-Curable Castor Oil Alkyd Resins Modified by Boron

Amardip Murlidhar Patil

amardipmpatil007@gmail.com

Kavayitri Bahinabai Chaudhari North Maharashtra University https://orcid.org/0000-0003-1836-6150

Madhuri P. Shimpi

Abdul Ahad

Ravindra R. Mahajan

Research Article

Keywords: UV curing, Boron acrylate, Biobased coating, Fatty amide, Monoglyceride

Posted Date: November 3rd, 2026

DOI: https://doi.org/10.21203/rs.3.rs-11375348/v1

License: This work is licensed under a Creative Commons Attribution 4.0 International License.
Read Full License

Study of High-Performance Protective Coatings of Bio-Based UV-Curable Castor Oil Alkyd Resins Modified by Boron

Madhuri P. Shimpi[1], Abdul Ahad[1], Ravindra R. Mahajan[2], Amardip M. Patil[1*]

[1]School of Chemical Sciences, Kavayitri Bahinabai Chaudhari North Maharashtra University Jalgaon, MS, 425001

[2]Deparment of Chemical Engineering, National Institute of Technology, Warangal, Telengana, 506004

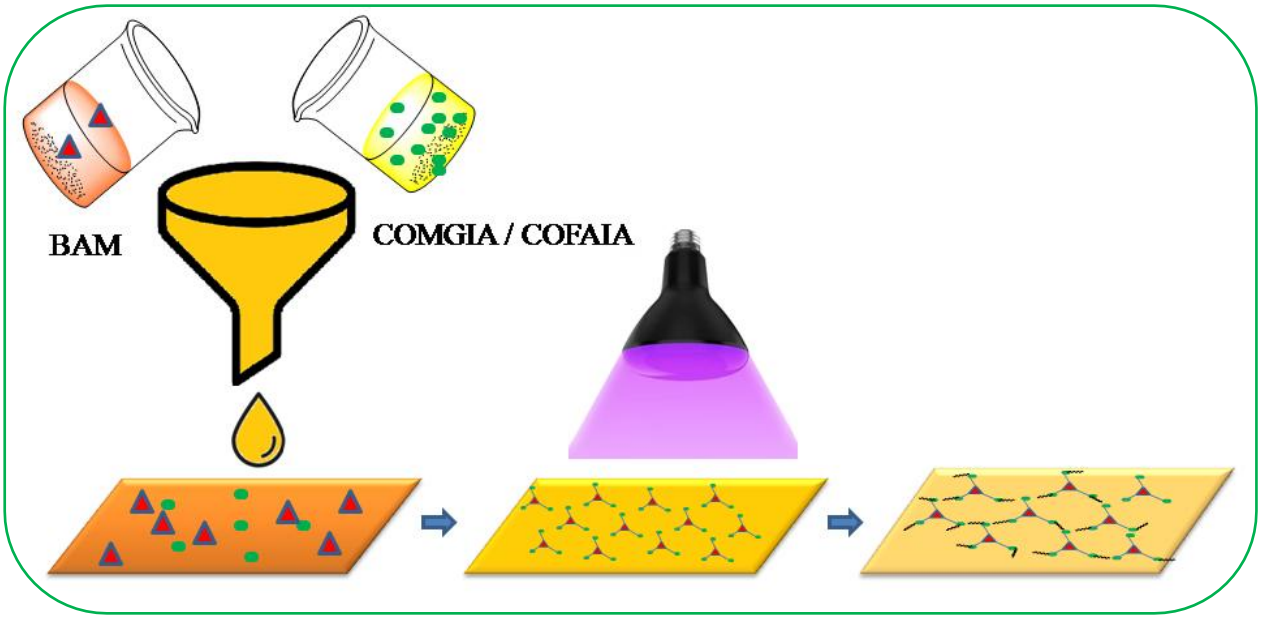
(*Corresponding Author: amardipmpatil007@gmail.com)

Abstract

In this current research, castor oil based fatty amide (COFA) and monoglyceride (COMG) were synthesized separately in the laboratory and subsequently reacted with itaconic acid to produce alkyd resins named as COFAIA and COMGIA, respectively. Afterwards, a boron based triacrylate monomer, (borane-triyltris(oxy))tris(ethane-2,1-diyl) (BAM) was prepared via esterification of boric acid and hydroxyethylacrylate (HEA), in a molar ratio of 1:3 using p-toluene sulphonic acid (pTSA) as a catalyst. Structural determination of synthesized materials COFAIA, COMGIA and BAM were done by Fourier transform Infrared Spectroscopy (FTIR) and Nuclear Magnetic Resonance (NMR).Then, using synthesized materials, various UV curable coating formulations were prepared by blending varying compositions of COFAIA or COMGIAwith BAM (0 to 5% in w/w). These compositions were coated as a film on mild steel and wood panels and cured under UV radiations. The cured coatings were evaluated for different properties by performing various tests such as cross-cut adhesion, pencil hardness, gloss test, impact resistance, scratch resistance, and stain test. Chemical resistance was evaluated by immersion method in 2N NaOH, 2N HCl, xylene, and water while anticorrosion property was determined in 3.5% NaCl solution. Thermal stability of synthesized compounds of COFAIA, COMGIA and BAM were studied by thermogravemetric analysis (TGA). Surface morphology and crystallanity of synthesized coating films were studied by scanning electron microscopy (SEM) and X-ray diffraction (XRD) analysis. Also, stain property of coatings was carried on coated wood panel. The results show that BAM incorporated UV curable films display superior performance by enhancing studied properties for their coating applications.

Keywords: UV curing, Boron acrylate, Biobased coating, Fatty amide, Monoglyceride

Graphical Abstract



1. Introduction

As need of eco-friendly coatings rises, the bio-based materials have become increasingly important[1-3]. Various renewable resources (vegetable oils, nutshells, carbohydrates, natural rubber, proteins and other bio-based materials) have been used for the improvement of coating materials[4]. Bio-based coatings have special properties over conventional petroleum-based coatings for instance fast curing, low energy requirement, low toxicity, biodegradability, better environmental compatibility as well as they are cost effective and easily available[5-7]. Therefore, bio-based coatings are receiving increasing attention in last decades [8]. Among the different renewable resources, vegetable oils, polysaccharides, pectin etc are being used for the preparation of bio-based UV-curable resins[9-11]. These materials can be modified into UV-curable coatings with good performance and potential applications in various coating. Vegetable oils (castor, palm, soya, bean linseed, sunflower, cotton seed, neem, karanja, coconut etc.) are effortlessly accessible and renewable comparatively low cost resources obtained from different oilseeds [12-25] Among these, castor oil is non edible vegetable oils, bearing an important hydroxyl- functional groups which is suitable for chemical modification and allows its use in different polymeric materials such as coatings, adhesives and polyurethane foams[13][14]. In recent years, castor oil has been widely investigated as a renewable starting material for the preparation of bio-based UV-curable coatings applications [15].

UV curing is an efficient technique in which liquid oligomers and multifunctional monomers are rapidly converted into a cross-linked polymer network by exposure to UV radiation[16]. This method has gained importance in industrial applications such as adhesive, polymer nanocomposites, and protective coatings because it provides faster curing than thermal curing methods, also reduce the use of volatile organic solvents, which makes the process more environmentally friendly [17-18].

Numerous researchers worldwide are investigating the different kinds of UV-curable resins that have different individuality like self-healing, flexibility, recyclability, solvent-free, improved hydrophobicity, thermal stability, good optical, adhesion, hardness, abrasion resistance, and mechanical qualities[19-27]. Chen et al. developed a fully bio-based, solvent- and photoinitiator-free UV-curable coating with flame-retardant and UV-triggered self-healing properties. The prepared coatings exhibited excellent thermal stability, solvent resistance, recyclability, and multifunctional performance, making them promising for sustainable advanced coating applications[28]. The UV-curable epoxidized soybean oil acrylates were developed by Attia and coworkers for coating which were reinforced with silane-modified Al_2O_3 nanoparticles. They have found that coatings were exhibited excellent corrosion protection, inhibition efficiency up to 99% and significantly improved barrier performance on steel surfaces[5]. Mustapha and co-workers has developed modified UV-curable epoxidized palm oil polyurethane acrylate coatings with acrylation-thiol. They have found that the UV curing time was reduced by 30 s at the optimum 4 phr loading while improving crosslinking density and coating properties[29]. Sesia et al. incorporated tannic acid as a natural additive into bio-based UV-curable epoxy coatings to improve their adhesion to steel substrates. They have observed that the incorporation of tannic acid significantly improve the adhesion of the UV-cured coatings while maintaining good coating performance[30]. Onen et al. developed the soybean oil-based UV curable coatings for aluminum alloys containing phosphorus. They have reported that UV-cured coatings exhibited excellent adhesion, improved corrosion resistance, and enhanced coating performance, demonstrating their potential as sustainable protective coatings[31]. Żyłka et al. has investigated and studied the functional properties of UV-curable epoxy coatings containing natural plant-based fillers. In their study researchers have reported that the modified coatings exhibited good mechanical performance together with enhanced

antibacterial activity, demonstrating the potential of natural additives in UV-curable coating systems[32-34].

In recent years, bio-based materials and polyurethane acrylate have been studied for developing flame-retardant UV-curable coatings by adding suitable flame-retardant compounds or applying a protective flame-retardant coating on the surface [35-41].

In the present study, castor oil-based monoglyceride and castor oil-based fatty amide was utilized as a sustainable feedstock for the synthesis of bio-based UV-curable resins. The boron-based flame-retardant additive was incorporated into the UV-curable coating formulations, and the resulting coatings were evaluated for their physicochemical, mechanical, thermal, and flammability properties.

2. Experimental

2.1. Materials

The raw materials such as Castor Oil, Glycerol, Itaconic acid, p-Toluene sulphonic acid (pTSA), Hydroquinone (HQ) and Ethyl Methyl Ketone were adopted from Loba Chemie Pvt. Ltd. The catalyst dibutyltin dilaurate (DBTDL) was obtained from TCI Pvt. Ltd. Boric acid was obtained from Spectrochem Pvt. Ltd. Mumbai (India). The cross-linker isophorone diisocyanate (IPDI), 1-Hydroxycyclohexyl phenyl ketone (photoinitiator) and 2-Hydroxyethyl acrylate (HEA) were acquired from Sigma Aldrich, Pvt. Ltd. The chemical calcium oxide (CaO), diethanolamine, sodium methoxide, toluene, and xylene were purchased from Qualligen Chemicals Pvt. Ltd. All the chemicals during the research work were used without purification.

2.2. Synthesis of Castor oil based monoglyceride (COMG)

The castor oil based monoglyceride (COMG) was synthesized by the reaction of castor oil (36.8 g, 0.1 M) and glycerol (8.5 g, 0.2 M) using calcium oxide (0.5 g) as a catalyst. All the required amount of reaction materials were charged into a three-necked round bottom

flask which was equipped with an overhead mechanical stirrer, thermometer and condenser. The reaction mixture was heated at 120º C with continuous stirring for 3 h. The formation of COMG was confirmed by dissolving the obtained product in methanol [43-44].

2.3. Synthesis of COMG based polyester polyol

The COMG based polyester polyol was prepared by reacting COMG (30 g) with itaconic acid (6.3 g) in the presence of a catalyst pTSA (0.8 g) and add HQ (0.1g) as an inhibitor. The necessitated amounts of materials were mixed in a three-necked round bottom flask equipped with an overhead mechanical stirrer, thermometer and condenser. The reaction mixture was heated with continuous stirring at 120-140ºC for 3h. The progress of the reaction was monitored by checking acid value after one hour interval and stopped when the acid value reached 10 mg of KOH/ gram of sample[1]. The synthesis process has been shown in figure 1.

2.4. Synthesis of Castor oil based fatty amide (COFA)

The castor oil based fatty amide (COFA) was synthesized by reacting castor oil (46.35 g) with diethanolamine (15.75 g) using sodium methoxide (0.6 g) as a catalyst. The reaction was carried out in a 250 mL three necked round bottom flask equipped with an overhead stirrer, thermometer, dropping funnel and condenser. The flask was placed in an oil bath and the reaction mixture was stirred at 80º C for 15 min under nitrogen atmosphere. Castor oil was then added slowly to the reaction mixture over a period of 20 min with continuous stirring, while the temperature was gradually increased to 120º C. The reaction mixture was maintained at 120º for a further 3 h with continuous stirring. The formation of fatty amide was confirmed by thin layer chromatography (TLC). After cooling, the product was dissolved in diethyl ether and washed with 15% aqueous sodium chloride solution. The organic layer was dried using anhydrous sodium sulfate, and the solvent was removed using a rotary vacuum evaporator to obtain the castor oil based fatty amide[44].

2.5 Synthesis of COFA based polyester polyol

The fatty amide based polyester polyol was prepared by reacting COFA (20 g) with itaconic acid (4.03 g) using pTSA (0.8 g) as a catalyst and HQ (0.3 g) as an inhibitor. The required amounts of reaction materials fatty amide (COFA), itaconic acid, pTSA and HQ were added and heated at 140 ºC upto 3 h in a three necked round bottom flask equipped with an overhead mechanical stirrer, thermometer and condenser. The improvement of the reaction was monitored by measuring the acid value at one hour intervals and the reaction was stopped when the acid value reached upto 10 mg KOH/g of sample. The synthesis procedure has been shown in figure 2.

2.6 Synthesis of Boron acrylate monomer

Boron acrylate monomer (BAM) was prepared by reacting boric acid (5.05 g) with 2-hydroxyethyl acrylate (HEA) (19.41 g) in the presence of p-toluene sulphonic acid (pTSA 0.5 g) as a catalyst and a small amount of hydroquinone (HQ) as an inhibitor. The reaction mixture was heated and stirred at 120º C in a 100 mL two necked round bottom flask equipped with a Dean-Stark apparatus and condenser under reflux for 3 h. After completion of the reaction, the solvent was removed using a rotary vacuum evaporator. The obtained BAM was an orange colored liquid with a yield of 99%. The overall reaction scheme is show in figure 3 [45].

2.7 Synthesis of UV Curable resins from COMGIA and COFAIA

The UV curable resins were prepared by a two step process at 70ºC by using IPDI (8.892 g, 0.04 mol), HEA (5.2 g, 0.04 mol) and COMGIA (1 eq.mol) in the presence of DBTDL (0.3% w, 0.072 g) catalyst. In the first step, IPDI (8.892 g, 0.04mol), DBTDL (0.072 g), and hydroquinone (0.029 g) were taken in a three-necked round bottom flask fitted with a mechanical stirrer, reflux condenser and thermometer. HEA (5.2 g, 0.04mol) was then added slowly to the reaction mixture over a period of 30 min with continuous stirring. In second

step, the resulting (IPDI+HEA) mixture was reacted with COMGIA (5.25 g, 0.0025 mol) at 70 °C (figure 1). The same procedure was followed for the preparation of the COFAIA based UV curable resin (figure 2).

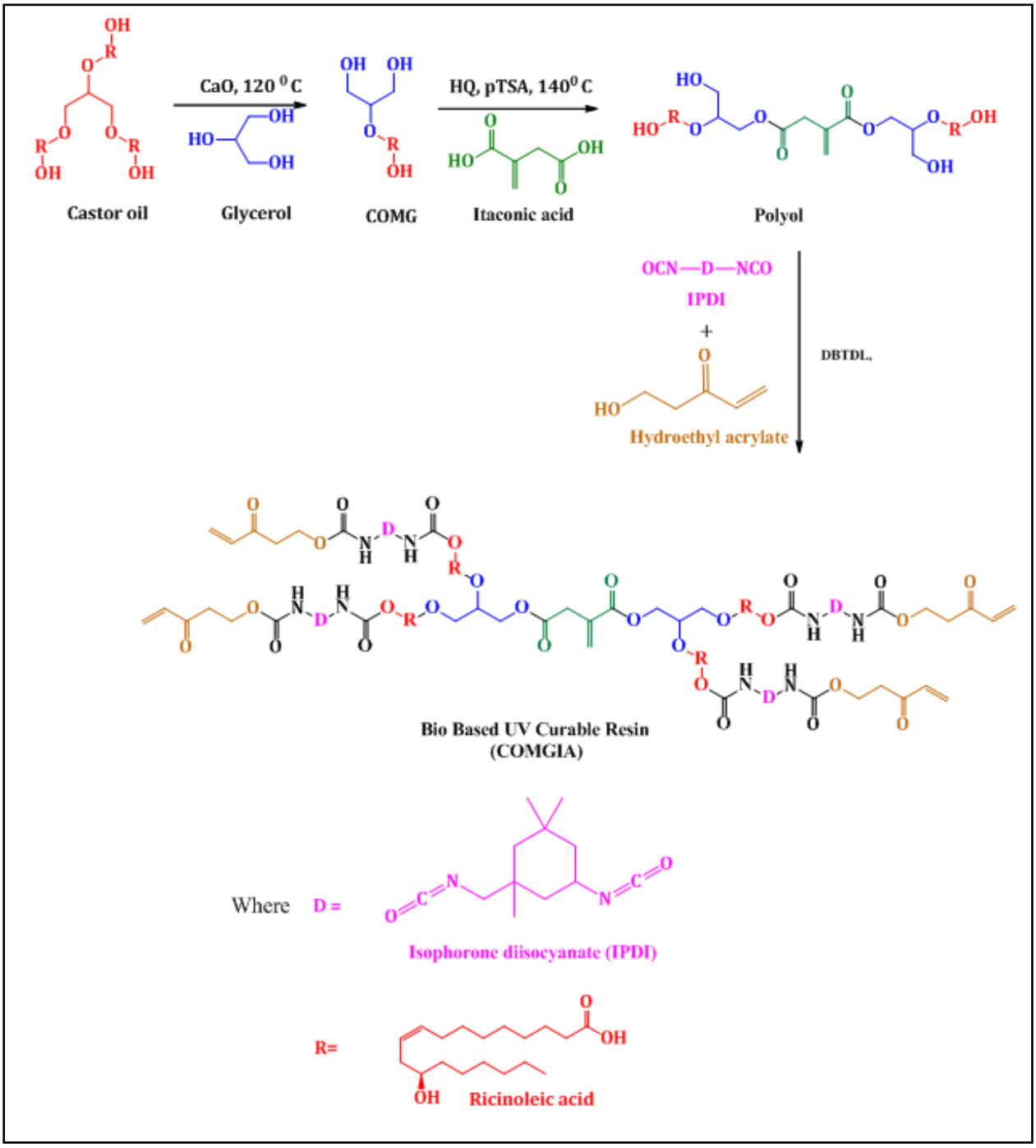


Figure 1. Synthesis of Castor oil based COMGIA resin

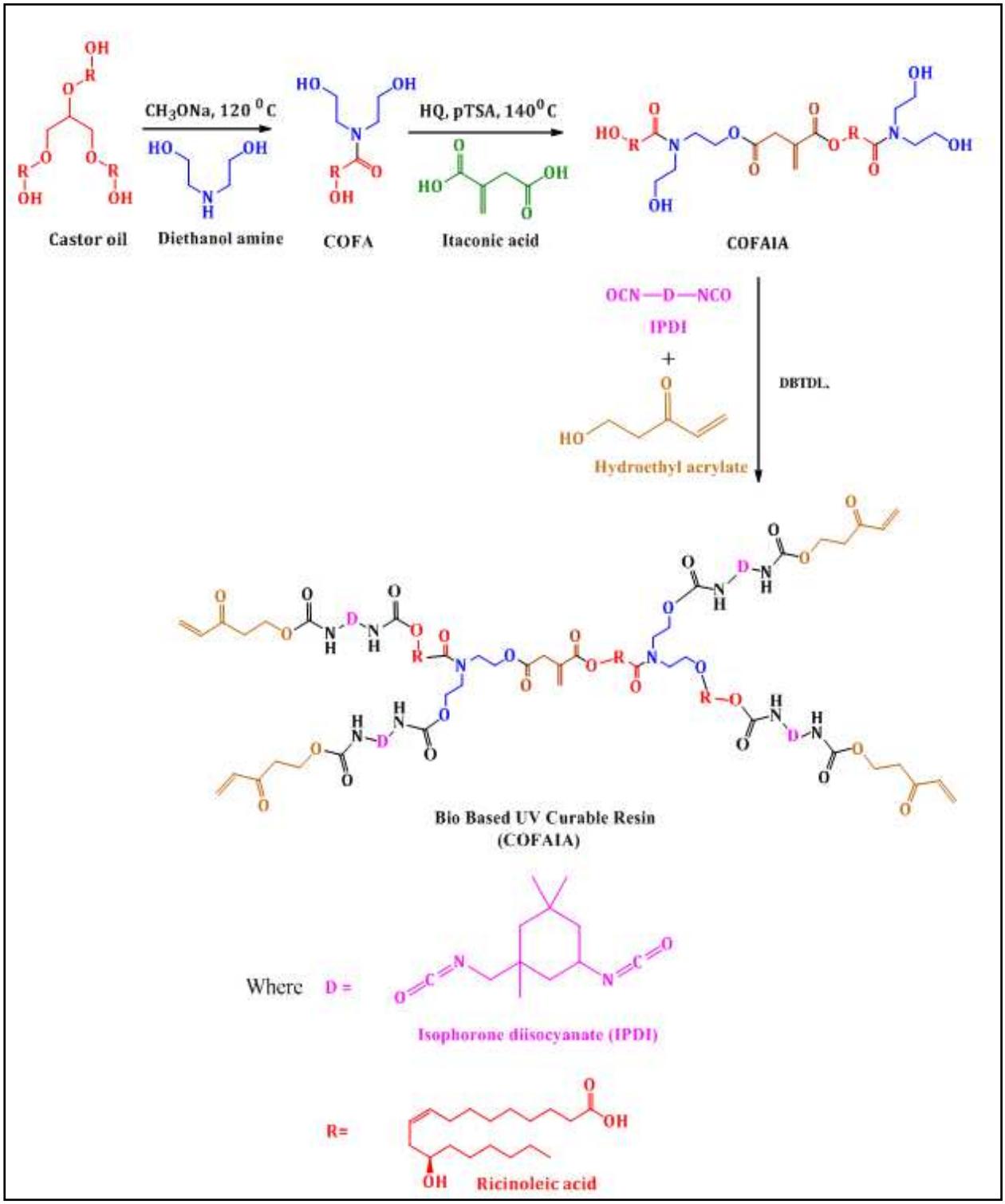


Figure 2.Synthesis of fatty amide based polyol

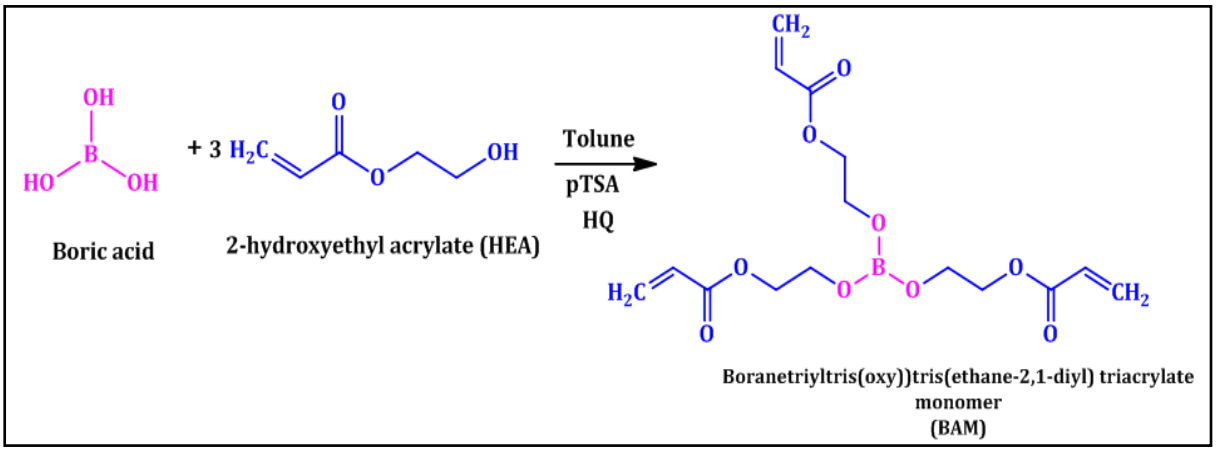


Figure 3. Synthesis of Boron acrylate monomer (BAM)

2.7 Preparation of UV- Curing panels

The various UV-curable coating formulations were prepared using COMGIA resin (1 g), BAM (1–5% w/w), and a photoinitiator (3% w/w) dissolved in a mixed solvent system of methyl ethyl ketone (MEK) and xylene. The formulations containing COMGIA and BAM were designated as COMGIA 0% BAM, COMGIA 1% BAM, COMGIA 2% BAM, COMGIA 3% BAM, COMGIA 4% BAM, and COMGIA 5% BAM, respectively. Similarly, formulations based on COFAIA resin containing varying concentrations of BAM were prepared and coded as COFAIA 0% BAM, COFAIA 1% BAM, COFAIA 2% BAM, COFAIA 3% BAM, COFAIA 4% BAM, and COFAIA 5% BAM, respectively. The prepared formulations were applied on mild steel panels, glass substrates and wood surfaces using a brush. The coated substrates were then exposed to UV radiation using a 4 kW UV lamp with a wavelength range of 300-400 nm for 30-35 s. The UV exposure resulted in the formation of fully cured coating films.

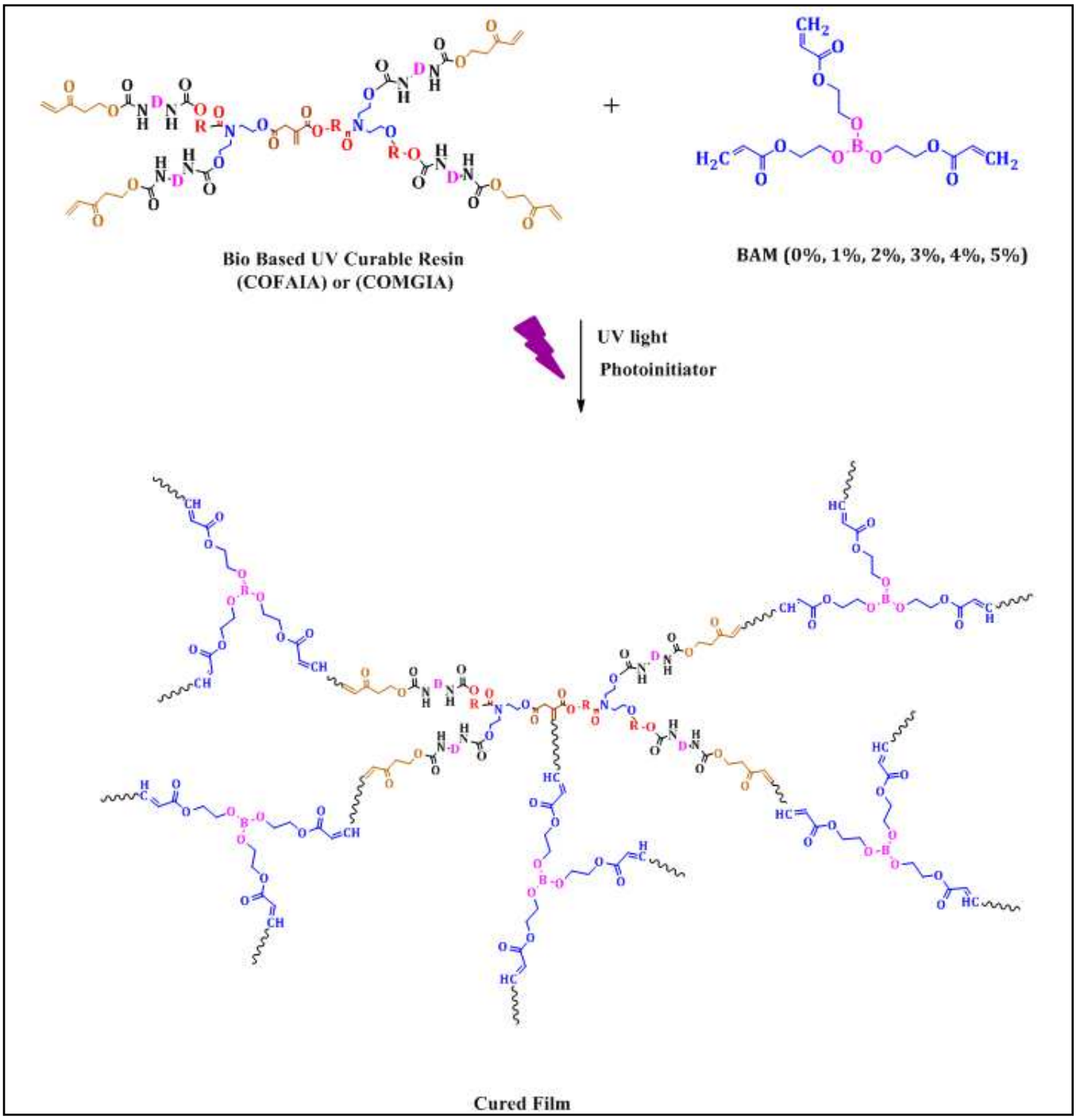


Figure 3. UV cured film of COFAIA or COMGIA

2.8. Characterizations

2.8.1. End group analysis of COMGIA and COFAIA

The end group analysis of the COMGIA and COFAIA compounds were determined in terms of hydroxyl and acid values according to ASTM D1957-86 and ASTM D1980-87, respectively.

$$Acid\ Value = \frac{56.1 \times \text{volume of KOH consumed} \times \text{exact concentration of the KOH solution}}{\text{weight of the resin sample in grams}} \quad \text{----------(Eq.1)}$$

$$Hydroxyl\ Value = \frac{56.1 \times \text{volume of KOH consumed} \times \text{exact concentration of the KOH solution}}{\text{weight of the resin sample in grams}} - Acid\ Value \text{ ---(Eq.2)}$$

Also, the C=C double bond content of the prepared compounds was determined from the iodine value using ASTM D-5768.

$$Iodine\ Value = \frac{12.69 \times (B - S) \times N}{W} \quad \text{----------(Eq.3)}$$

In the iodine value determination, 'B' represents the volume in mL of sodium thiosulfate ($Na_2S_2O_3$) solution used for the blank titration. While 'S' represents the volume in mL $Na_2S_2O_3$ solution was used in the back titration. The term '**N**' denotes the normality of the $Na_2S_2O_3$ solution and "W" is the weight of the sample in grams. The factor '12.69' is a conversion factor, calculated from the molecular weight of iodine (126.9 g/mol) and the fact that iodine reacts with sodium thiosulfate in 1:2 ratio.

2.8.2. FTIR and NMR studies of COMGIA, COFAIA and BAM:

The presence of functional groups (hydroxyl, carboxyl and C=C groups) and the structural determination of COMGIA, COFAIA and BAM compounds, were characterized by fourier transform infrared spectroscopy (FTIR) (Bruker Alpha-II instrument) and nuclear magnetic resonance (NMR) spectroscopy (Bruker Avance III HD 400 MHz spectrometer). The NMR spectra were recorded in chloroform ($CDCl_3$) as the solvent and tetramethylsilane (TMS) as the standard.

2.8.3. Gloss

By using the calibrated digital gloss meter (BYK Additives & Instruments), the gloss of the COMGIA-BAMs and COFAIA-BAMs coating panels were determined at an angle of 95º.

2.8.4. Flexibility

A conical mandrel instrument (Raj Scientific Co., Mumbai, India) was used for the determination of the flexibility of the COMGIA-BAMs and COFAIA-BAMs coating films applied on mild steel panels.

2.8.5. Pencil hardness

The determination of pencil hardness of the COMGIA-BAMs and COFAIA-BAMs coating panels were carried on a pencil hardness tester (BYK Additives & Instruments) according to ASTM D3363[46].

2.8.6. Cross-cut adhesion

The adhesion of the UV cured COMGIA-BAMs and COFAIA-BAMs coating to the substrate was evaluated using a cross-cut adhesion tester (Elcometer, Model 107) according to ASTM D3359 [47].

2.8.7. Impact resistance

The tubular impact tester was used for the determination of impact resistance on coating mild steel panels. In this test, an indenter weighing of 1.36 lb weight was dropped from different heights, starting from 5 inches and gradually increasing up to 100 inches, onto the coated panels. The test was continued until visible damage, such as cracking peeling or detachment of the coating films were observed. The impact resistance was determined based on the maximum height at which the coating remained intact without visible cracking or deformation. All the UV cured COMGIA-BMAs and COFAIA-BAMs coating panels were evaluated using tubular impact tester.

2.8.8. Chemical resistance

The immersion method was used for the determination of the chemical resistance of UV cured COMGIA-BAMs and COFAIA-BAMs in different chemical solutions, including acid (2N HCl), alkali (2N NaOH), 3.5% NaCl solution, water and xylene at room temperature for 7 days. The coated panels were visually examined at 24 h intervals and the changes on the coating surface, such as loss of gloss, swelling, deterioration and formation of cracks were observed and recorded.

2.8.9. Stain resistance

The stain resistance was performed on the UV- cured COMGIA-BAMs and COFAIA-BAMs coated wood panels according to ASTM D3023-98. The various staining material was used such as turmeric water, ketchup, permanent parker, ink, lipstick, oil (mustard oil).

2.8.10. Flammability

The flammability of UV-cured COMGIA-BAMs and COFAIA-BAMs coating films was approved out according to ASTM D635.

2.8.11. Thermal gravimetric analysis

The thermal stability of the coating films (COMGIA-BAMs and COFAIA-BAMs) was determined by thermogravemetric analyzer (TGA). During this process, an approximately 3to 5 mg of each sample was heated from 40 to 700 °C at a constant heating rate of 10 °C/min under a nitrogen atmosphere.

2.8.12. Study of surface morphology

The surface morphology of the UV-cured COMGIA-BAMs and COFAIA-BAMs films were studied using field emission scanning electron microscopy (FESEM) (TESCAN VEGA 3 LMU).

2.8.13. X-ray diffraction study of coating films

X-ray diffraction (XRD) analysis was carried out to study the crystallanity of the UV-cured COMGIA-BAM and COFAIA-BAM films.

3. Results and discussion

3.1. End group analysis of COMGIA and COFAIA

The acid, hydroxyl and iodine values which are mentioned in Table 1, have more importance for evaluating the properties of the prepared resins as well as for coating. They are used as sign of the completion of reactions between MG or FA and itaconic acid.

Table 1 End group analysis

Sr. no.	Sample	Acid value (mg of KOH/g)	Hydroxyl value (mg of KOH/g)	Iodine value (I_2/100 g of sample)
1	COMGIA	10.6	246.9	197.5
2	COFAIA	10.4	233.5	178.3

3.2. Functional group analysis by FTIR

The functional groups present in the synthesized COFAIA, COMGIA and BAM were characterized using FTIR spectroscopy; the corresponding spectra are shown in Figure 5. The FTIR spectrum of BAM Figure 5 (a) shows the carbonyl (C=O) stretching band obtained at 1722 cm^{-1}. The band observed at 2979 cm^{-1} due to the presence of CH_2 groups was confirmed. The peak at 1132 cm^{-1} is pointed to the C=C group unsaturation. The peak at 784cm^{-1} indicates the -B-O-C- stretching. The FTIR spectrum of COMGIA Figure 5 (b) shows a peak at 1720 cm^{-1} due to the carbonyl group (C=O), while the C=C bending vibration was observed at 1193 cm^{-1}. The peak observed at 2873 cm^{-1} and 2990 cm^{-1} in

FTIR due to the $–CH_2-$ group stretching. The FTIR spectrum of COFAIA Figure 5 (c) shows a peak at 1209 cm^{-1} , indicating the presence of C=C groups. The peak at 1720 cm^{-1} was assigned to the carbonyl (C=O) group, while the band at 1635 cm^{-1} was attributed to the amide (–NH–CO–) group. The peak obtained at 2870 cm^{-1} and 2988 cm^{-1} in FTIR due to the $–CH_2-$ group stretching.

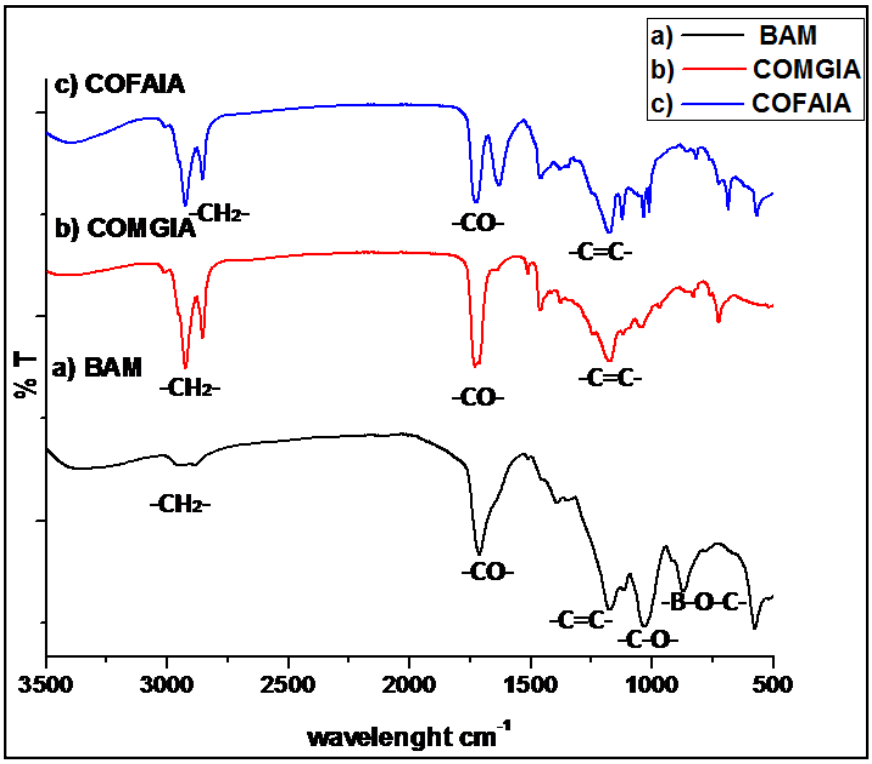


Figure 4. FT-IR spectra of a) BAM b) COFAIA c) COMGIA

3.3. ^{1}H NMR spectral study of COFAIA, COMGIA and BAM

The figure 6 of ^{1}HNMR spectra of COMGIA shows peaks and different types of proton. The peak at 0.9 ppm corresponds to terminal methyl group ($-CH_3$). The peak obtained between 1.3 to 1.6 ppm due to the methylene group ($-CH_2$). The peaks between 1.9 to 2.3 ppm regarding to $-CH_2-C=C-$ and $–CH_2-CO-$ groups, respectively. The peaks ranging from 4.2 to 4.8 ppm indicated the proton attached to carbon with hydroxyl group (H-C-OH). The band obtained at 3.7 ppm due to the proton of hydroxyl group (-OH). The proton on alkene group

(–CH=CH–) obtained at the band 5.3 to 5.7 ppm. The figure 7 shows the ^{1}HNMR spectra for COFAIA in which chemical shifts observed for COFAIA at of 0.9 ppm for methyl group (-CH_3). The chemical shifts ranging from 1.3 to 1.5 ppm indicates methylene group (–CH_2) in fatty chain. The chemical shifts ranging from 1.8 to 2.3 ppm due to the protons in –CH_2–C=C– and –CH_2–C=O groups. The chemical shift at 4.1 to 4.3 ppm indicates the protons –CH_2–O– and –CH_2–N– groups. The chemical shift at 3.5 ppm corresponding to –OH group. The chemical shift between 5.2 to 5.4 ppm corresponds to protons on unsaturation (–CH=CH–). The 1HNMR spectra of BAM is shown in figure 8

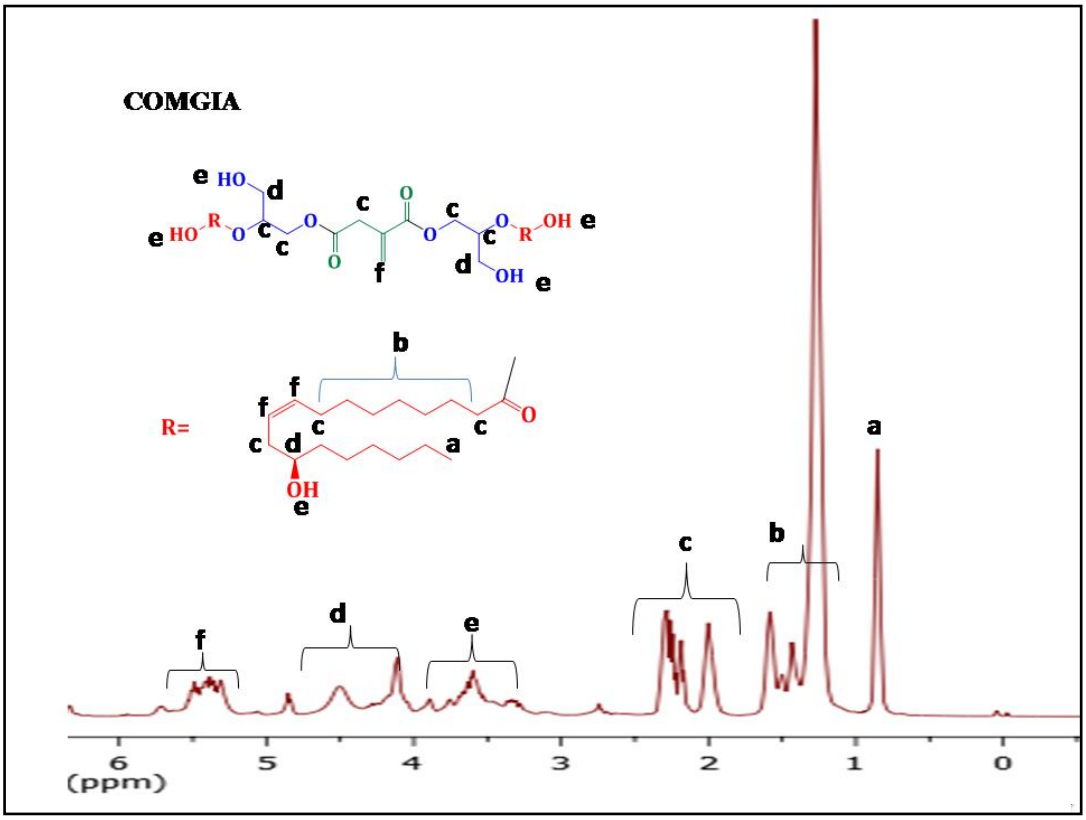


Figure 6. ^{1}H NMR of COMGIA

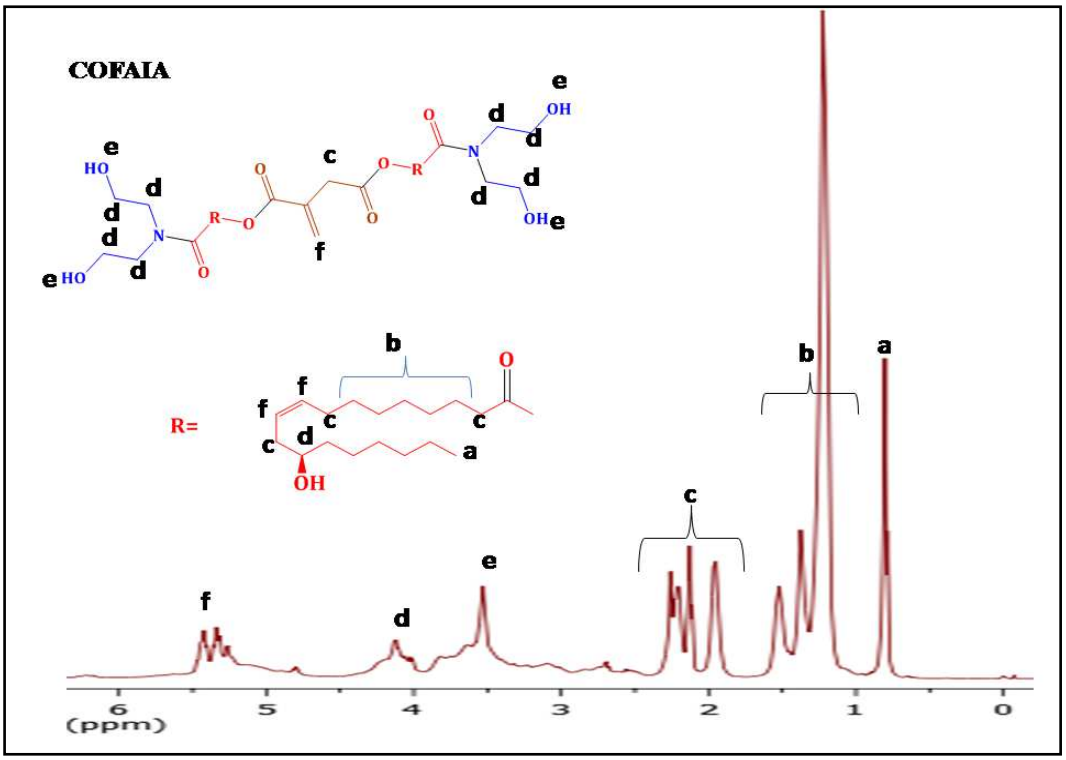


Figure 7.1H NMR of COFAIA

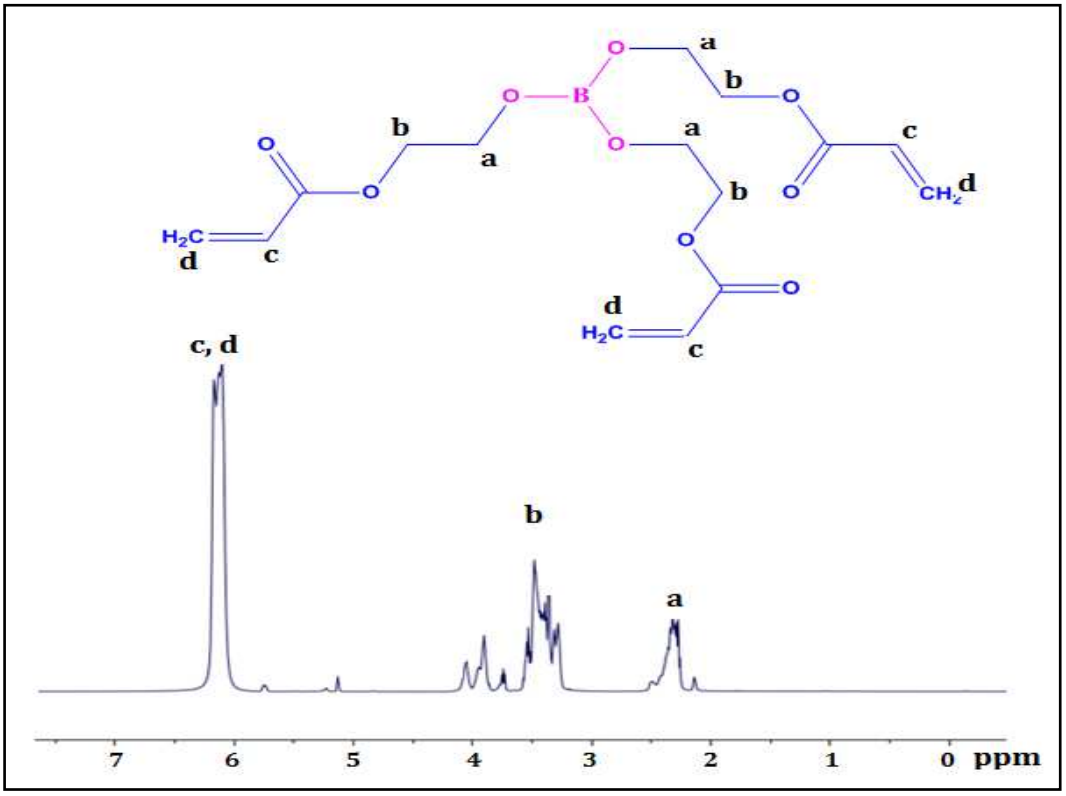


Figure 5.^{1}H NMR of BAM

3.4. Mechanical properties

3.4.1. Gloss

Gloss in a coating refers to the reflectivity of the sample surface. The results of gloss test of COFAIA-BAMs and COMGIA-BAMs are mentioned in Table 2 and Table 3, respectively.The results show that the gloss of the coatings decreased with increasing BAM content in the coating formulation.

3.4.2. Cross-cut adhesion test

The cross-cut adhesion test was used to evaluate the adhesion of the coatings to the mild steel panels. The coatings showing no detachment within the square lattice or along the cut edges were considered to have good adhesion strength. The cross-cut adhesion results of the COFAIA-BAMs and COMGIA-BAMs coatings are presented in Table 2 and Table 3. The adhesion of the coatings increased with increasing BAM concentration in the formulation. This improvement may be attributed to the increased crosslinking density of the coating network with increasing BAM content.

3.4.3. Pencil hardness test

The pencil hardness results of the COFAIA-BAMs coatings are shown in Table 2. The coating of COFAIA 0% BAM, COFAIA 1% BAM, COFAIA 2% BAM and COFAIA 3% BAM, were passed up to 3H, 4H, 4H and 4H respectively, while coatings of COFAIA 4% BAM and COFAIA 5% BAM were passed up to 6H, 6H respectively. Due to enhance the concentration of BAM in the coating of COFAIA 4% BAM and COFAIA 5%BAM showed better performance than lower concentration of BAM (Table 2). While in COMGIA-BAMs pencil hardness are shown in Table 3. COMGIA 0% BAM, COMGIA 1%BAM and COMGIA 2% BAM were passed up to 3H, 3H, and 4H, respectively. While coating of COMGIA3%BAM, COMGIA4%BAM and COMGIA5%BAM were all showed better performance due to BAM percentage and passed up to 6H respectively (Table 3).

3.4.4. Impact resistance

The impact resistance test was carried out to evaluate the ability of the coating films to resist cracking, peeling or detachment from the substrate under sudden deformation. The results presented in Table 2 and Table 3 show that the coating panels containing 0–4% BAM passed the impact resistance test, whereas the coatings containing 5% BAM failed. The failure at higher BAM concentration may be attributed to an increase in the brittleness of the coating film due to the higher BAM content.

3.4.5. Flexibility Test

The flexibility test was carried out to evaluate the ability of the coating films to with stand bending and deformation without cracking, peeling or loss of adhesion. As shown in Table 2 and Table 3, all the coating panels containing 0–4% BAM passed the flexibility test, whereas the coatings containing 5% BAM failed. The failure at higher BAM concentration may be attributed to an increase in the brittleness of the coating films with increasing BAM content.

Table 2 Mechanical properties of COFAIA-BAMs

Sr.No.	Sample	Gloss at 95^0	Cross-cut adhesion	Pencil hardness	Impact resistance	Flexibility test
1	COFAIA 0% BAM	104.59	1B	3H	Pass	Pass
2	COFAIA 1% BAM	109.81	2B	4H	Pass	Pass
3	COFAIA 2% BAM	101.83	2B	4H	Pass	Pass
4	COFAIA 3% BAM	98.63	3B	4H	Pass	Pass
5	COFAIA 4% BAM	96.78	3B	6H	Pass	Pass
6	COFAIA 5% BAM	95.82	4B	6H	Fail	Fail

Table 3 Mechanical properties of COMGIA-BAMs

Sr.No.	Sample	Gloss at 95^0	Cross-cut adhesion	Pencil hardness	Impact resistance	Flexibility test
1	COMGIA 0% BAM	105.78	1B	3H	Pass	Pass
2	COMGIA 1% BAM	104.06	1B	4H	Pass	Pass
3	COMGIA 2% BAM	96.47	2B	4H	Pass	Pass
4	COMGIA 3% BAM	94.21	3B	6H	Pass	Pass
5	COMGIA 4% BAM	94.16	4B	6H	Pass	Pass
6	COMGIA 5% BAM	89.99	4B	6H	Fail	Fail

3.4.4. Chemical resistance and Immersion Test

The chemical resistance of the UV-cured COMGIA-BAM and COFAIA-BAM coatings was evaluated against 2 N HCl, 2 N NaOH, 3.5% NaCl solution, water and xylene for up to 168 h. All COFAIA-BAM and COMGIA-BAM coatings showed loss of gloss and deterioration of the coating film after exposure to 2 N HCl. This may be attributed to the reaction of the acidic solution with the ester groups present in the coating. In 2 N NaOH solutions, all COMGIA-BAM coatings were affected, whereas the COFAIA-BAM coatings showed partial deterioration. The COMGIA-BAM coatings showed better chemical resistance towards 3.5% NaCl solution, water and xylene compared with the COFAIA-BAM coatings. The observations are presented in Table 4 and Table 5 and Figure 9 and Figure 10.

Table 4 Immersion test of COFAIA-BAMs

Sr.no.	Samples\ chemicals	2N HCl	2N NaOH	3.5% NaCl	Water	Xylene
1	COFAIA 0% BAM	a	b	e	d	e
2	COFAIA 1% BAM	a	c	c	e	e
3	COFAIA 2% BAM	a	c	b	b	d
4	COFAIA 3% BAM	a	e	d	b	e
5	COFAIA 4% BAM	a	c	d	c	e
6	COFAIA 5% BAM	a	c	d	e	e
Note : a = loss of gloss, b = film swelling, c = slight cracking, d = partial removal of the film, e = unaffected.						

Table 5 Immersion test of COMGIA-BAMs

Sr. no.	Samples\ chemicals	2N HCl	2N NaOH	3.5% NaCl	Water	Xylene
1	COMGIA 0% BAM	a	d	e	d	e
2	COMGIA 1% BAM	a	b	d	e	e
3	COMGIA 2% BAM	a	a	b	e	e
4	COMGIA 3% BAM	a	c	d	b	e
5	COMGIA 4% BAM	a	b	d	b	e
6	COMGIA 5% BAM	a	b	d	e	e
Note : a = loss of gloss, b = film swelling, c = slight cracking, d = partial removal of the film, e = unaffected.						

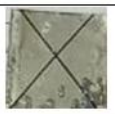
Sr.no.	Samples\chemicals	2N HCl	2N NaOH	3.5% NaCl	Water	Xylene
1	COFAIA 0%BAM					
2	COFAIA 1%BAM					
3	COFAIA 2%BAM					
4	COFAIA 3%BAM					
5	COFAIA 4%BAM					
6	COFAIA 5%BAM					

Figure 6. Images of immersion test of COFAIA-BAMs

Sr.no.	Samples\chemicals	2N HCl	2N NaOH	3.5% NaCl	Water	Xylene
1	COMGIA 0%BAM					
2	COMGIA 1%BAM					
3	COMGIA 2%BAM					
4	COMGIA 3%BAM					
5	COMGIA 4%BAM					
6	COMGIA 5%BAM					

Figure 7. Images of immersion test of COMGIA-BAMs

3.4.5. Stain resistance:

The stain resistance test was carried out to evaluate the ability of the UV-cured coatings to resist staining by different substances and to determine their ease of cleaning. The stain resistance of the UV-cured wood coatings was evaluated according to ASTM D3023-98 using permanent marker, ink, turmeric water, lipstick, ketchup and oil. The staining agents were placed on the coated surface and kept for 24 h before cleaning. Ketchup stains were completely removed by washing with water, while lipstick, permanent marker, ink and oil stains were completely removed after cleaning with ethanol, indicating excellent stain resistance of the UV-cured coatings. In the case of turmeric water, the stain intensity decreased after cleaning, although slight residual staining was observed. This may be due to the presence of curcuminoids, which are hydrophobic polyphenolic compounds that can interact with the coating surface, making turmeric stains relatively difficult to remove [15]. Among the two modifiers, fatty amide (FA) exhibited slightly better stain resistance than monoglyceride (MG), particularly against lipstick and permanent marker at lower modifier contents. However, both FA- and MG-based coatings achieved excellent stain resistance toward all staining agents at higher modifier contents. The improved stain resistance may be attributed to the formation of a densely crosslinked three-dimensional network during UV curing, which can restrict the penetration of staining molecules into the coating matrix. As a result, the UV-cured coatings showed good resistance to both water-based and oil-based staining agents. The comparative stain resistance results are presented in Table 6 and Table 7, while the corresponding observations are shown in Figure 11 and Figure 12.

Table 6 . Stain resistance of COMGIA-BAMs

Sr. no.	Samples	Lipstick	Turmeric +water	Ketchup	Ink	Permanent marker	Oil
1	COMGIA 0% BAM	3	4	5	5	3	5
2	COMGIA 1% BAM	4	5	5	5	4	5
3	COMGIA 2% BAM	5	5	5	5	5	5
4	COMGIA 3% BAM	5	5	5	5	5	5
5	COMGIA 4% BAM	5	5	5	5	5	5
6	COMGIA 5% BAM	5	5	5	5	5	5
Note: 1= stain does not removed, 2=partially removed, 3=slightly, invisible, 4=invisible, 5=excellent.							

Table 7 Stain resistance of COFAIA-BAMs

Sr. no.	Samples	Lipstick	Turmeric + water	Ketchup	Ink	Permanent marker	Oil
1	COFAIA 0% BAM	4	4	5	5	4	5
2	COFAIA 1% BAM	5	4	5	5	4	5
3	COFAIA 2% BAM	5	5	5	5	5	5
4	COFAIA 3% BAM	5	5	5	5	5	5
5	COFAIA 4% BAM	5	5	5	5	5	5
6	COFAIA 5% BAM	5	5	5	5	5	5
Note: 1= stain does not removed, 2=partially removed, 3=slightly, invisible, 4=invisible, 5=excellent.							

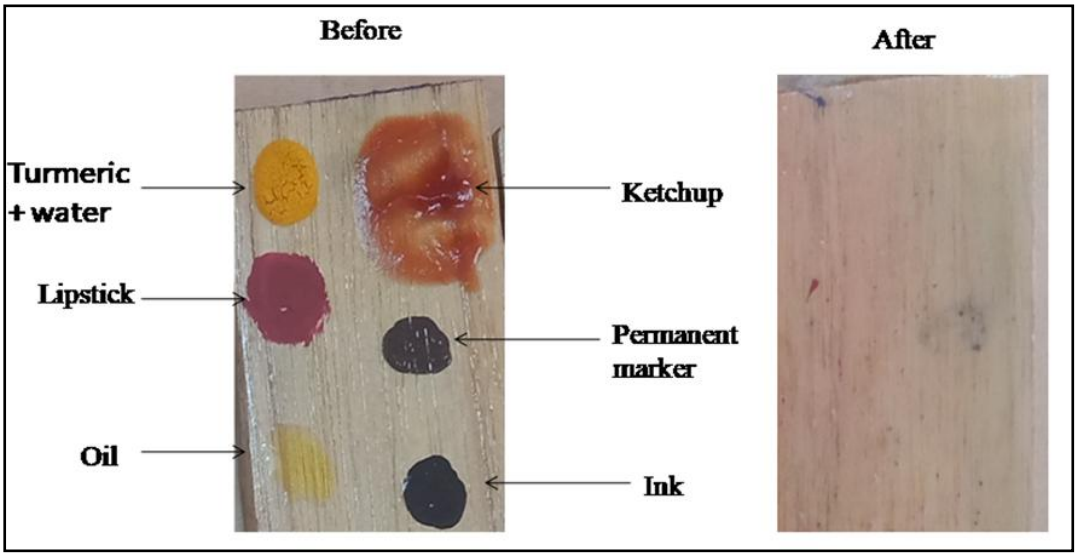


Figure 8. Stain resistance of COFAIA-BAMs

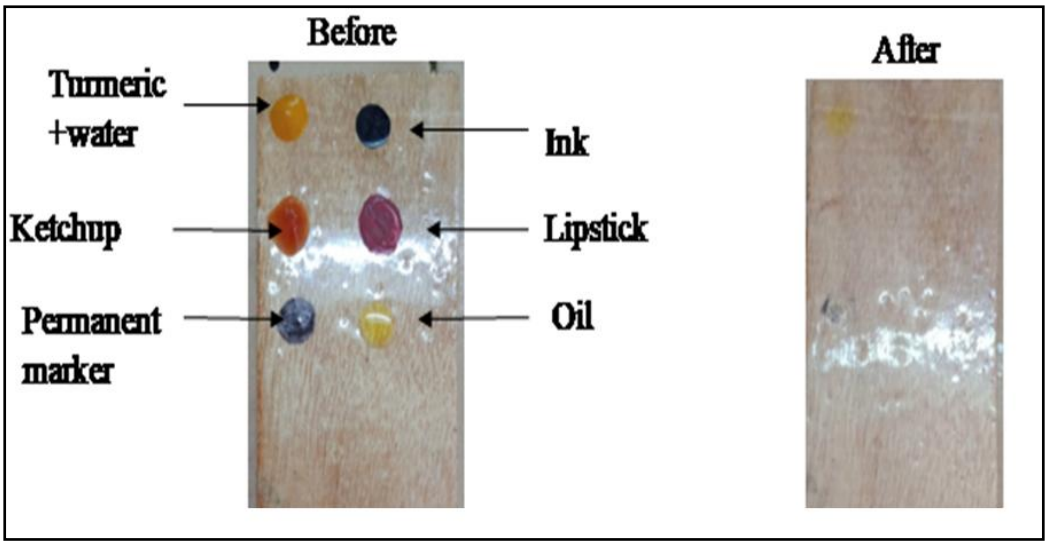


Figure 9. Stain resistance of COMGIA-BAMs

3.5. Flammability test

The linear burning rate (LBR) of the film samples was evaluated using the ASTM D635 horizontal flammability test[48]. Film samples of (40 to 50 mm) were prepared for both the film COFAIA BAM and COMGIA BAM, show in Figure 13.

LBR (mm/min) was calculated using the equation 4

$$LBR = \frac{\text{Burning distance}(mm)\times 60}{\text{Time taken }(s)} \quad \text{----------(Eq.4)}$$

Where, the burning distance is the fixed distance. Time taken is the duration for the flame to travel this distance. The factor '60' is a unit conversion factor into minutes because the burning rate is reported in mm per minute, shown in Table 8 and Table 9 and observations in Figure 13. From the observations of flame retardancy test, it was determined that as the amount of BAM increases in coatings the flame retardancy increases.

Table 8 Flammability test of COFAIA-BAMs

Sr. no.	Samples	Burn distance (mm)	Burning time(s)	LBR (mm/min)
1	COFAIA 0% BAM	40	20	120
2	COFAIA 1% BAM	40	23	104.3
3	COFAIA 2% BAM	40	27	88.8
4	COFAIA 3% BAM	40	30	80.8
5	COFAIA 4% BAM	40	34	70
6	COFAIA 5% BAM	40	40	60

Table 9 Flammability test of COMGIA-BAMs

Sr. no.	Samples	Burn distance (mm)	Burning time(s)	LBR (mm/min)
1	COMGIA 0% BAM	40	15	160
2	COMGIA 1% BAM	40	20	120
3	COMGIA 2% BAM	40	24	100
4	COMGIA 3% BAM	40	28	85.7
5	COMGIA 4% BAM	40	32	75
6	COMGIA 5% BAM	40	34	70.5

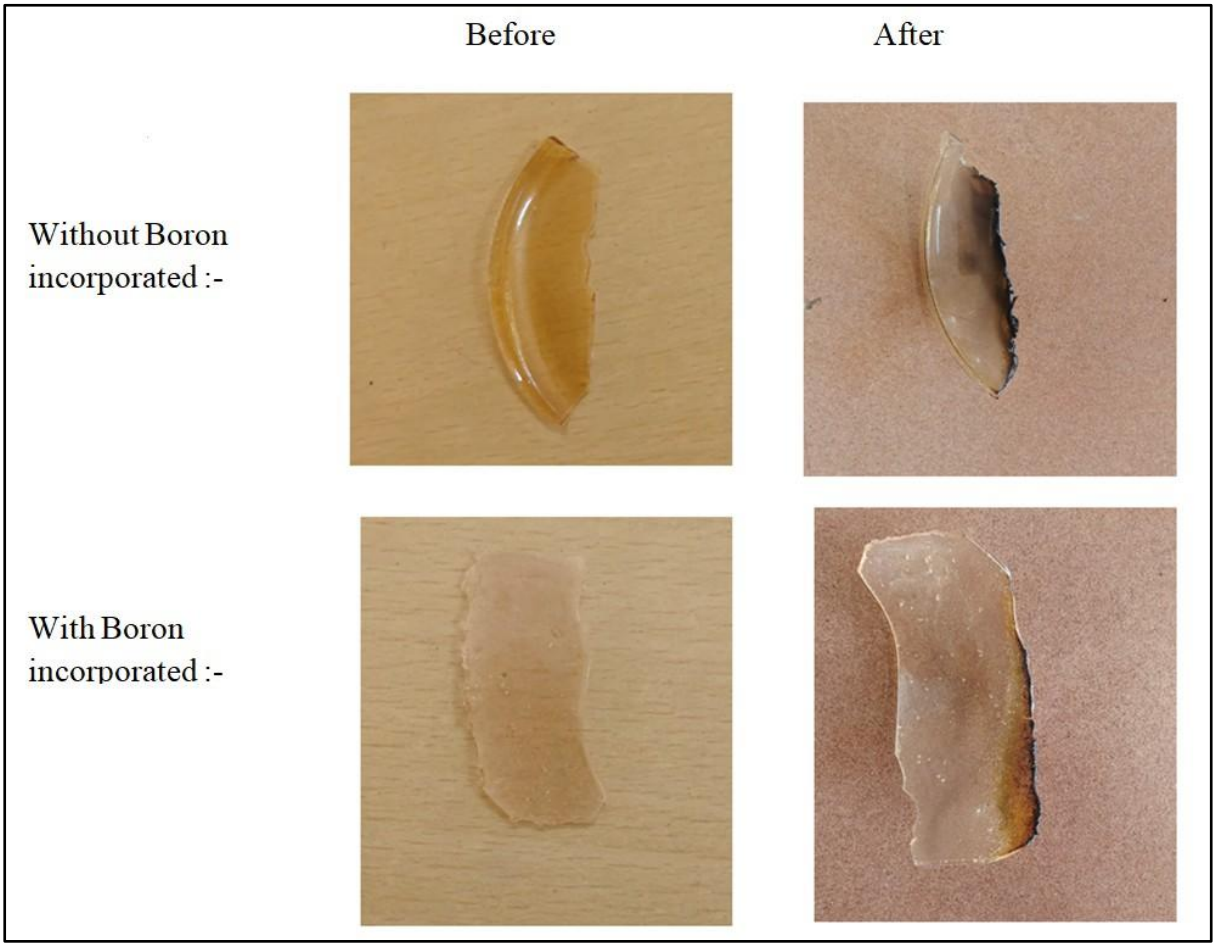


Figure 13. Flammability test

3.6. Thermal study of COFAIA-BAMs and COMGIA-BAMs films

The thermal behaviour of the COFAIA-BAM and COMGIA-BAM coatings was studied using thermogravemetric analysis (TGA). All the polyurethane coatings showed a three-step degradation pattern [23]. The incorporation of BAM improved the thermal stability of both coating systems, as indicated by the gradual increase in the onset decomposition temperature, temperature at 50 wt.% weight loss (T_{50}), and char residue with increasing BAM content. For the COMGIA-BAM coatings, the onset decomposition temperature increased from 203 to 257 °C, the T_{50} increased from 376 to 392 °C, and the char residue increased from 1.359 to 3.754 mg. Similarly, for the COFAIA-BAM coatings, the onset decomposition temperature T_{ON} increased from 211 to 252 °C, the T_{50} increased from 358 to 393 °C, and the char residue increased from 0.403 to 1.557 mg. The improved thermal stability with increasing BAM content may be attributed to the formation of a more densely crosslinked polymer network during UV curing. The 5 wt.% BAM formulations showed the highest thermal stability in both coating systems. Overall, the COMGIA-BAM coatings showed slightly higher thermal stability than the COFAIA-BAM coatings, as indicated by the higher onset decomposition temperature and greater char residue obtained for the COMGIA-BAM system. The TGA results are presented in Table 10 and Table 11, Figure 14 and Figure 15.

Table 10 Thermal parameters of COMGIA-BAMs coatings

Sr. no.	Sample	Onset decomposition temperature (T_{ON}) in ^{0}C	50% wt loss temperature (T_{50}) in ^{0}C	Weight(mg) residue at 650 ^0C
1	COMGIA 0% BAM	203	376	1.359
2	COMGIA 1% BAM	218	379	1.557
3	COMGIA 2% BAM	220	383	2.042
4	COMGIA 3% BAM	225	384	2.181
5	COMGIA 4% BAM	233	385	3.487
6	COMGIA 5% BAM	257	392	3.754

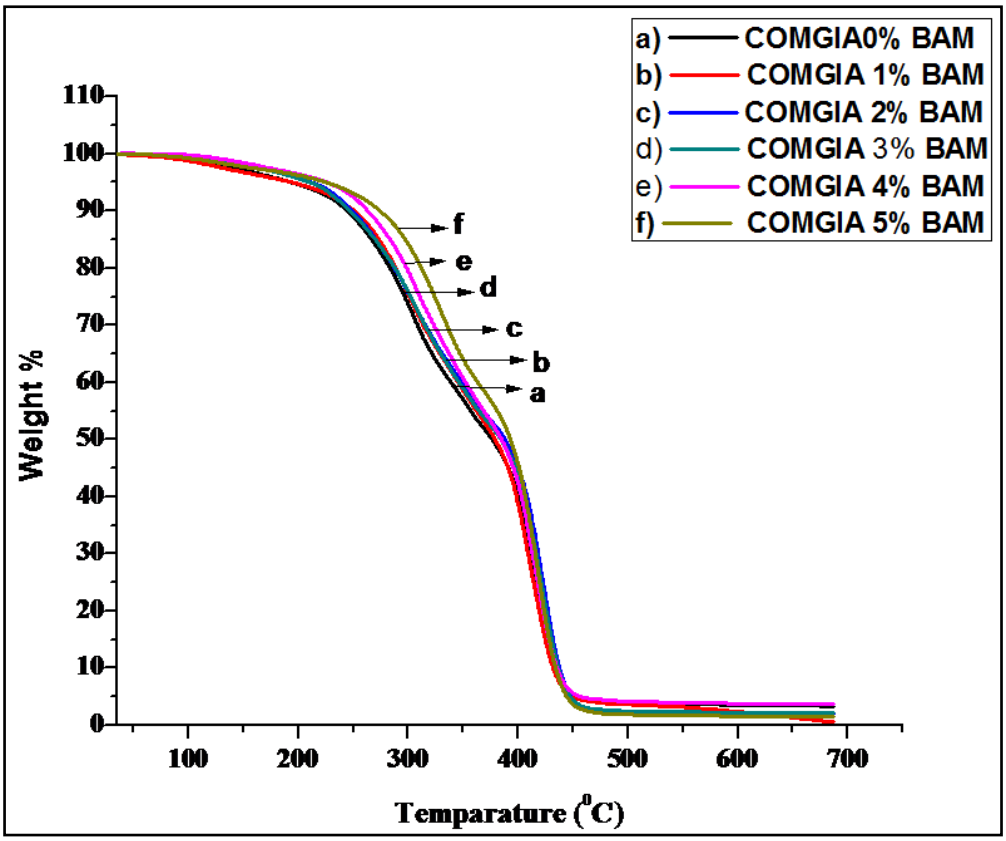


Figure 14. Thermo gravimetric curves of COMGIA-BAMs

Table 11 Thermal parameters of COFAIA-BAMs coatings

Sr. no.	Sample	Onset decomposition temperature (T_{ON}) in ^0C	50% wt loss temperature (T_{50}) in ^0C	Weight(mg) residue at 650 ^0C
1	COFAIA 0% BAM	211	358	0.403
2	COFAIA 1% BAM	221	372	1.293
3	COFAIA 2% BAM	229	377	1.333
4	COFAIA 3% BAM	231	381	1.351
5	COFAIA 4% BAM	239	386	1.441
6	COFAIA 5% BAM	252	393	1.557

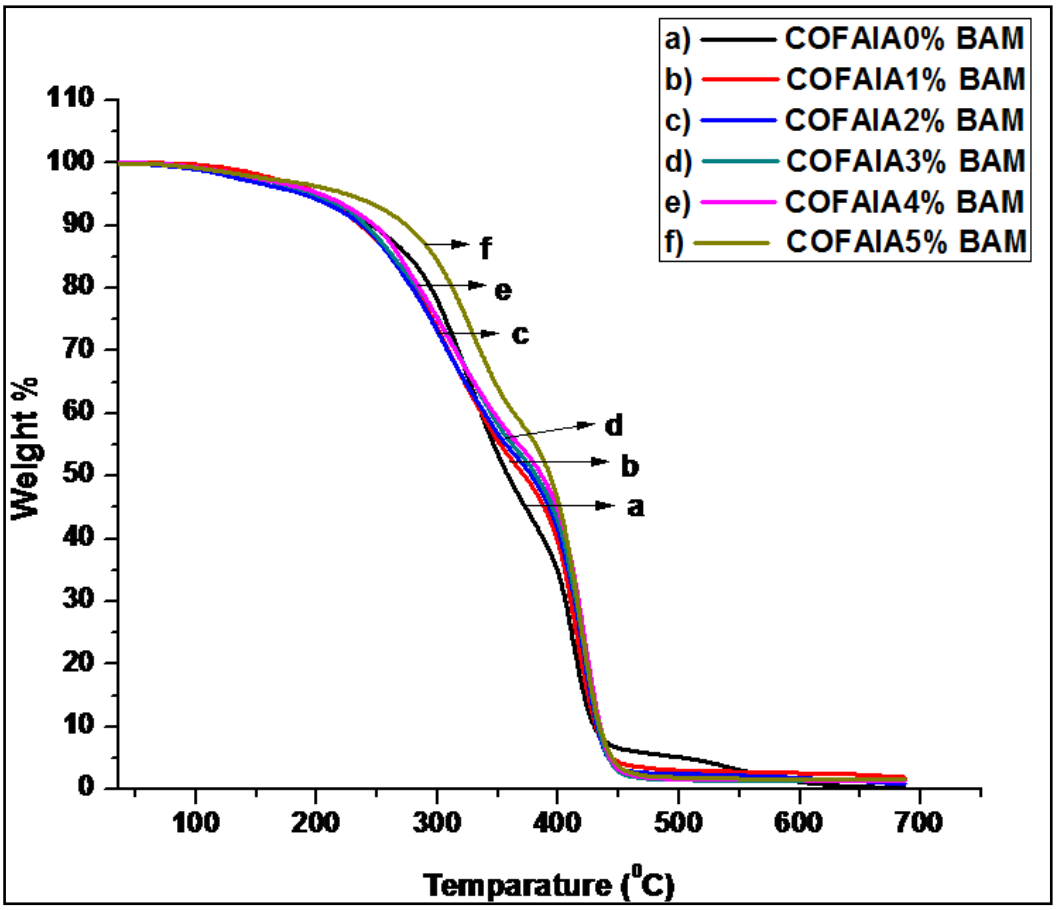


Figure 15. Thermo gravimetric curves of COFAIA-BAMs

3.7. Surface morphology of coatings

The surface morphology of the UV-cured coatings was studied using scanning electron microscopy (SEM). All the coating films were observed to be free from trapped air bubbles and pinholes during film casting[49]. The SEM images showed some patched regions on the coating surfaces, which may be related to the non-uniform distribution of rigid and flexible segments, except for the COMGIA 1% BAM and COFAIA 1% BAM coatings. The COFAIA-BAM coatings (Figure 17) exhibited comparatively smoother and more homogeneous surfaces than the COMGIA-BAM coatings (Figure 16). The COMGIA-BAM coatings showed slight surface roughness and some agglomerated domains at higher BAM concentrations. The relatively uniform morphology of the COFAIA-BAM coatings may be associated with the molecular structure of the fatty amide-based resin, which can provide

better intermolecular interactions and compatibility within the UV-cured urethane-acrylate network.

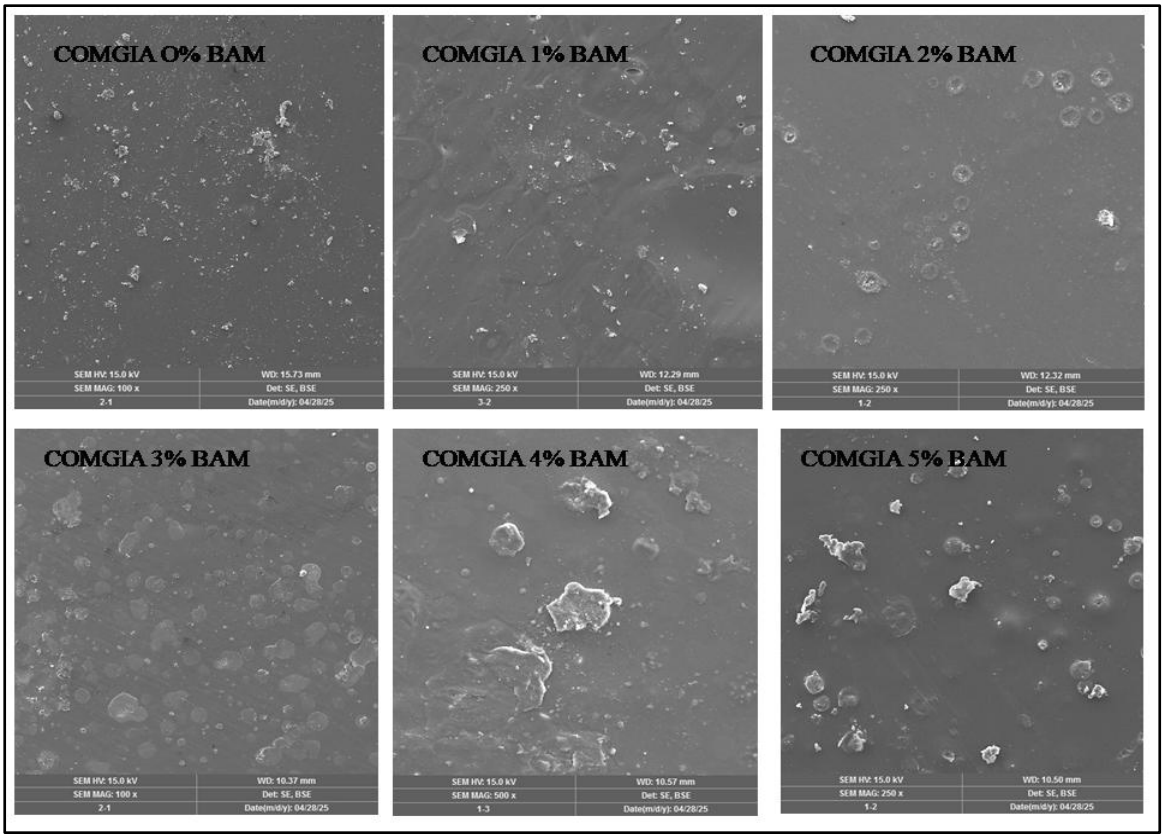


Figure 10. SEM images of COMGIA-BAMs

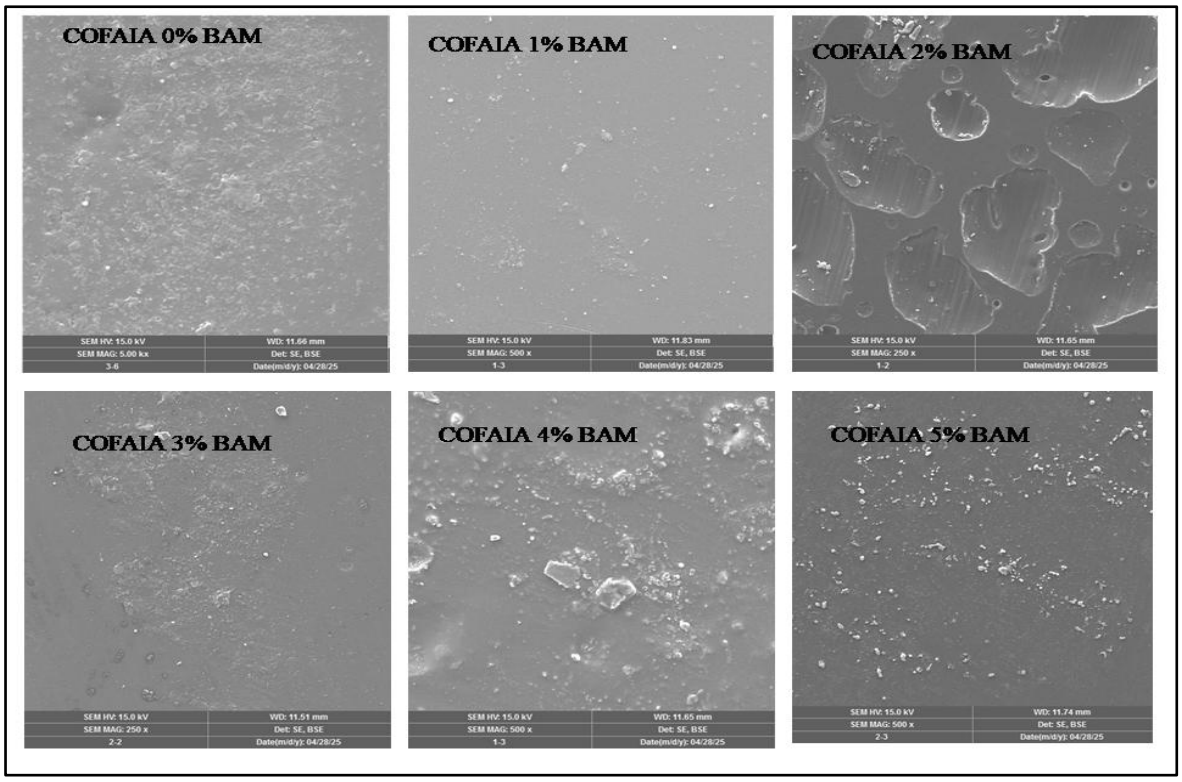


Figure 17. SEM images of COFAIA-BAMs

3.8. Study of crystallinity of the coatings by XRD

X-ray diffraction (XRD) was used to study the crystalline or amorphous nature of the UV-cured coatings by analyzing the diffraction patterns of the samples [50]. The XRD patterns of the COMGIA-BAM and COFAIA-BAM coatings are shown in Figure 18 and Figure 19, respectively. The absence of sharp and distinct diffraction peaks in the XRD patterns indicates that all the prepared coatings are predominantly amorphous in nature.

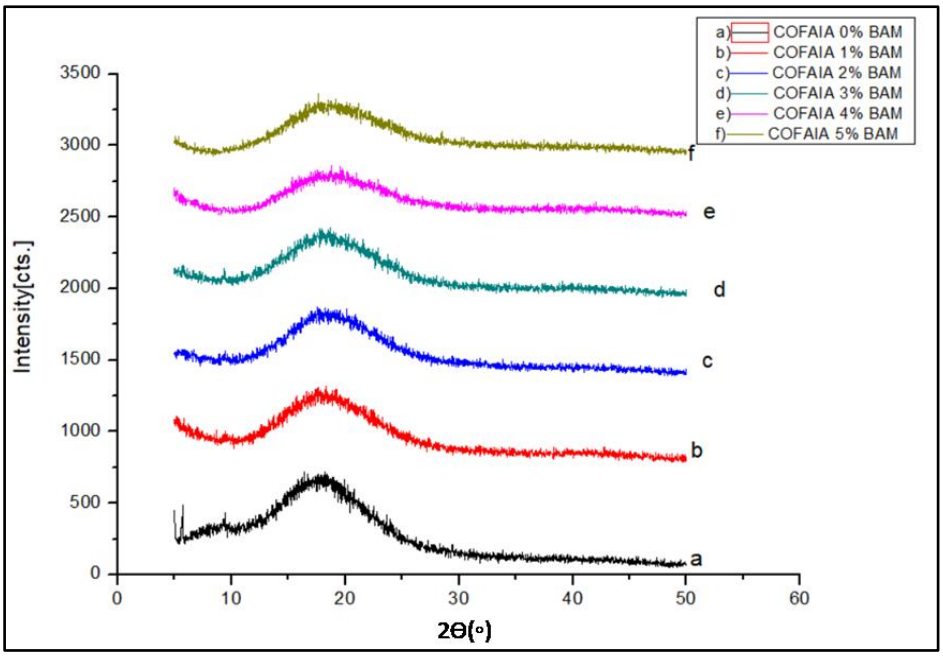


Figure 18. XRD study of COFAIA-BAMs coatings

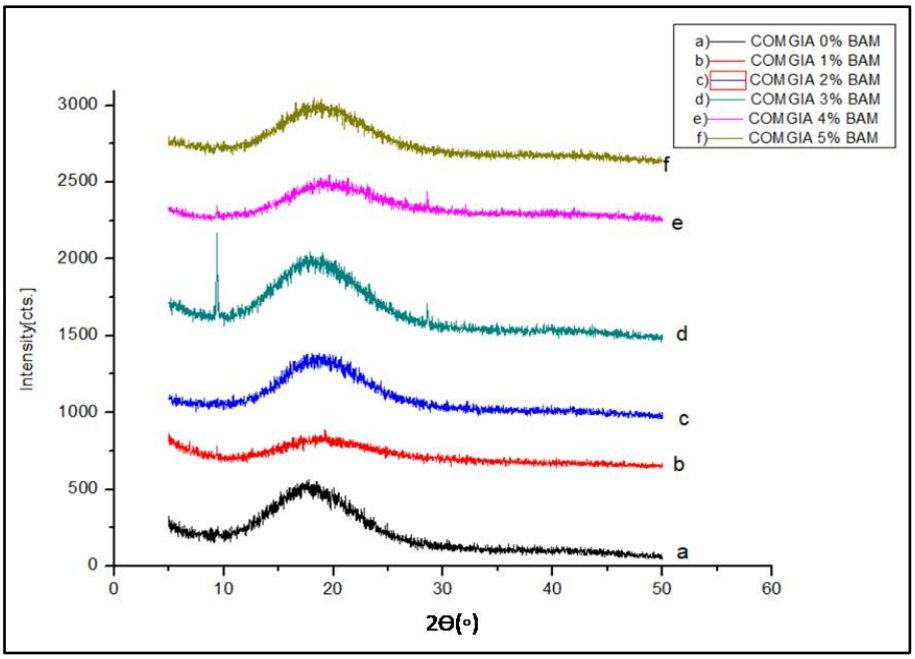


Figure 19. XRD study of COMGIA-BAMs coatings

4. Conclusions

The current study we can conclude that the synthesis of castor oil-based UV-cured resins, COMGIA and COFAIA, were effectively completed. The boron acrylate monomer (BAM) was synthesized and incorporated in various amounts into the UV-curable coatings. The coating properties of the UV-cured coatings were evaluated and compared to their analogues. Among the COMGIA coatings, the COMGIA 4% BAM coating sample exhibited excellent coating properties, while among the COFAIA coatings, the COFAIA 4% BAM coating showed excellent coating properties. The COFAIA 5% BAM and COMGIA 5% BAM coatings demonstrated excellent chemical resistance. All coatings exhibited outstanding stain resistance. The thermal studies revealed that the thermal stability of the coatings increased with increasing BAM content; therefore, the COMGIA 5% BAM and COFAIA 5% BAM coatings showed better thermal stability. Furthermore, the flame-retardant performance evaluated by the LBR test improved with increasing BAM concentration in the coatings. The SEM analysis revealed a homogeneous and smooth surface morphology for COFAIA-BAM coatings, indicating proper distribution of BAM within the

coating matrix. In contrast, COMGIA-BAM coatings exhibited a slightly inhomogeneous surface morphology. The XRD spectra confirmed the crystalline nature of both COFAIA-BAM and COMGIA-BAM UV-cured coatings. Compared to their analogues, the COMGIA 4% BAM and COFAIA 4% BAM coatings generally exhibited superior coating and mechanical properties. Overall, the incorporation of BAM significantly enhanced the coating performance, thermal stability, and flame-retardant characteristics of the UV-cured coating systems.

Acknowledgements: The author gratefully acknowledges the technical and analytical support provided by the National Institute of Technology, Warangal, India, during this work. We appreciate the cooperation of Dr. Ravindra Mahajan, National Institute of Technology, Warangal, India

Funding: The authors did not receive financial support from any association for the submitted work.

Declarations of competing interests: The authors declare that they have no known competing financial interests or personal relationships that could have appeared to influence the work reported in this paper.

References:

[1] A. M. Patil, H. D. Jirimali, V. V Gite, and R. N. Jagtap, "Synthesis and performance of bio-based hyperbranched polyol in polyurethane coatings," *Prog. Org. Coatings*, vol. 149, p. 105895, 2020, doi: 10.1016/j.porgcoat.2020.105895.

[2] A. M. Patil, "Synthesis and characterization of bio-based polyester and polyamide from citric acid and mannitol," *Orient. J. Chem.*, vol. 34, no. 1, pp. 538–543, 2018, doi: 10.13005/ojc/340161.

[3] A. M. Patil, H. D. Jirimali, and R. N. Jagtap, "Pure and Applied Chemistry Study of coating performance of bio-based hyperbranched polyester polyol / graphene oxide composites in PU-coating," *J. Macromol. Sci. Part A*, vol. 0, no. 0, pp. 1–9, 2020, doi:

10.1080/10601325.2020.1826330.

[4] E. Nadim, I. Major, D. Devine, and P. Paraskar, “Biobased self-healing functional composites and their applications,” *J. Mater. Sci. Compos.*, vol. 6, 2025, doi: 10.1186/s42252-025-00065-x.

[5] M. Attia, M. B. I. Mohamed, M. A. Hegazy, M. M. Ghobashy, H. Abd El-Wahab, and F. Abdelhai, “Enhancing corrosion resistance with chemically modified aluminum oxide in UV-curable coatings applied to steel surfaces,” *Sci. Rep.*, vol. 15, pp. 1–21, 2025, doi: 10.1038/s41598-025-99898-6.

[6] L. Najera-losada, C. P. Narváez-rincón, A. Orjuela, J. Gomez-caturla, O. Fenollar, and R. Balart, “Plasticization of Polylactide Using Biobased Epoxidized Isobutyl Esters Derived from Waste Soybean Oil Deodorizer Distillate,” *J. Polym. Environ.*, vol. 33, pp. 125–144, 2025, doi: 10.1007/s10924-024-03415-1.

[7] T. J. Hammer, C. Pugh, and M. D. Soucek, “Photopolymerization kinetics of UV-curable polyester powder coatings containing urethane methacrylate reactive diluents,” *J. Coatings Technol. Res.*, vol. 22, no. 5, pp. 1791–1805, 2025, doi: 10.1007/s11998-025-01079-7.

[8] M. Yamamura, “Reaction-driven solvent transport in UV-curable phase-separating coatings,” *J. Coatings Technol. Res.*, vol. 20, no. 1, pp. 15–26, 2023, doi: 10.1007/s11998-022-00661-7.

[9] D. Yu, I. B. Basumatary, S. Kumar, F. Ye, and J. Dutta, “Chitosan modified with bio-extract as an antibacterial coating with UV filtering feature,” *Int. J. Biol. Macromol.*, vol. 230, p. 123145, 2023, doi: 10.1016/j.ijbiomac.2023.123145.

[10] C. P. Jim and J. A. Cecilia, “Chitosan : A Natural Biopolymer with a Wide and Varied Range of Applications,” *Molecules*, vol. 25, 2020, doi: 10.3390/molecules25173981.

[11] H. Shaghaleh, X. Xu, and S. Wang, “Current progress in production of biopolymeric materials based on cellulose, cellulose nanofibers, and cellulose derivatives,” *R. Soc. Chem.*, vol. 8, pp. 825–842, 2018, doi: 10.1039/c7ra11157f.

[12] A. Das, T. Ringu, S. Ghosh, and N. Pramanik, “A comprehensive review on recent advances in preparation, physicochemical characterization, and bioengineering applications of biopolymers,” *Polym. Bull.*, vol. 80, pp. 7247–7312, 2023, doi: 10.1007/s00289-022-04443-4.

[13] M. S. Gaikwad, V. V. Gite, P. P. Mahulikar, D. G. Hundiwale, and O. S. Yemul, “Eco-friendly polyurethane coatings from cottonseed and karanja oil,” *Prog. Org. Coatings*, vol. 86, pp. 164–172, 2015, doi: 10.1016/j.porgcoat.2015.05.014.

[14] R. Muller and G. Wilke, “Synthesis and radiation curing of acrylated castor oil glycerides,” *J. Coat. Technol. Res.*, vol. 11, no. 6, pp. 873–882, 2014, doi: 10.1007/s11998-014-9596-5.

[15] S. Potdar, S. Maiti, A. Ukirade, and R. Jagtap, “Bio-based interior UV-curable coating designed for wood substrates,” *J. Coatings Technol. Res.*, vol. 22, no. 1, pp. 239–254, 2025, doi: 10.1007/s11998-024-00970-z.

[16] J. Zhang, Q. Shang, Y. Hu, G. Zhu, J. Huang, and X. Yu, “Castor-oil-based UV-curable hybrid coatings with self-healing , recyclability , removability , and hydrophobicity,” *Prog. Org. Coatings*, vol. 165, p. 106742, 2022, doi: 10.1016/j.porgcoat.2022.106742.

[17] D. Wei, B. Liao, J. Huang, M. Zhang, and H. Pang, “Fabrication of castor oil-based hyperbranched urethane acrylate UV-curable coatings via thiol-ene click reactions,” *Prog. Org. Coatings*, vol. 135, pp. 114–122, 2019, doi: 10.1016/j.porgcoat.2019.05.039.

[18] M. Azani and A. Hassanpour, “UV-Curable Polymer Nanocomposites : Material Selection , Formulations , and Recent Advances,” *J. Compos. Sci.*, vol. 8, 2024, doi: 10.3390/jcs8110441.

[19] F. Gao *et al.*, “Properties of UV-cured self-healing coatings prepared with PCDL-based polyurethane containing multiple H-bonds,” *Prog. Org. Coatings*, vol. 113, pp. 160–167, 2017, doi: 10.1016/j.porgcoat.2017.09.011.

[20] H. Xiang *et al.*, “Effect of soft chain length and generation number on properties of flexible hyperbranched polyurethane acrylate and its UV-cured film,” *Prog. Org. Coatings*, vol. 114, pp. 216–222, 2018, doi: 10.1016/j.porgcoat.2017.10.019.

[21] J. Aizpurua, L. Martin, M. Fernández, A. González, and L. Irusta, “Recyclable, remendable and healing polyurethane/acrylic coatings from UV curable waterborne dispersions containing Diels-Alder moieties,” *Prog. Org. Coatings*, vol. 139, no. November 2019, 2020, doi: 10.1016/j.porgcoat.2019.105460.

[22] A. Condini, C. Trentalange, A. Giuliani, A. Cristoforetti, and S. Rossi, “Advancing corrosion protection in confined spaces: a solvent-free UV LED-curable coating for steel pipelines with enhanced barrier properties and harsh environment performance,” *J. Coatings Technol. Res.*, vol. 21, no. 6, pp. 2009–2022, 2024, doi: 10.1007/s11998-024-00950-3.

[23] M. Çınar, G. Çaylı, and S. Karataş, “Synthesis and characterization of

ureidopyrimidinone‐functionalized polyurethane acrylates and their hybrid nanocomposites for UV coating applications," *Polym. Bull.*, vol. 81, no. 12, pp. 11077–11105, 2024, doi: 10.1007/s00289-024-05226-9.

[24] Y. Zou, Y. Xia, and X. Yan, "Effect of Melamine Formaldehyde Resin Encapsulated UV Acrylic Resin Primer Microcapsules on the Properties of UV Primer Coating," *Polymers (Basel).*, vol. 16, no. 16, 2024, doi: 10.3390/polym16162308.

[25] L. Wu and Y. Zhang, "Study on the effect of reactive diluents on exothermic UV curable and coating films properties," *J. Phys. Conf. Ser.*, vol. 2680, no. 1, 2024, doi: 10.1088/1742-6596/2680/1/012043.

[26] Y. Zou, Y. Xia, and X. Yan, "Effect of UV Top Coating Microcapsules on the Coating Properties of Fiberboard Surfaces," *Polymers (Basel).*, vol. 16, no. 15, 2024, doi: 10.3390/polym16152098.

[27] A. R. Banan, "Solvent free UV curable waterborne polyurethane acrylate coatings with enhanced hydrophobicity induced by a semi interpenetrating polymer network," *Sci. Rep.*, vol. 15, no. 1, pp. 1–14, 2025, doi: 10.1038/s41598-025-04739-1.

[28] W. Chen, T. Huang, N. Zhang, A. Xi, and Y. Zeng, "A solvent- and photoinitiator-free strategy for bio-based UV-curable coatings with flame retardancy and UV-triggered self-healability," *Ind. Crops Prod.*, vol. 236, p. 121973, 2025, doi: 10.1016/j.indcrop.2025.121973.

[29] S. N. H. Mustapha, M. I. Mohamad Isa, M. S. Shamsuddin, R. Roslan, R. Mustapha, and M. J. Jalil, "Enhancing the Curing Efficiency and Physicochemical Properties of Acrylated Epoxidized Palm Oil Polyurethane Coatings via Double Acrylation-Thiol Modification," *J. Polym. Environ.*, vol. 33, no. 7, pp. 3368–3387, 2025, doi: 10.1007/s10924-025-03589-2.

[30] R. Sesia, A. G. Cardone, S. Ferraris, S. Spriano, and M. Sangermano, "Exploitation of tannic acid as additive for the adhesion enhancement of UV-curable bio-based coating," *Prog. Org. Coatings*, vol. 189, p. 108311, 2024, doi: 10.1016/j.porgcoat.2024.108311.

[31] H. A. Onen, Z. Yildiz, O. Gurer, and A. Gungor, "Development of sustainable bio-based photocurable coatings on aluminum alloy surfaces," *J. Coatings Technol. Res.*, vol. 23, no. 1, pp. 513–524, 2026, doi: 10.1007/s11998-025-01152-1.

[32] W. Żyłka, B. Pilch-Pitera, K. Krawczyk, E. Ciszkowicz, B. Grabowska, and A. Bobrowski, "UV Light-Curable Epoxy Coatings with Natural Plant-Based Fillers—

Evaluation of Antibacterial and Functional Properties," *Materials (Basel).*, vol. 18, no. 23, pp. 1–24, 2025, doi: 10.3390/ma18235464.

[33] S. Brannstrom, E. Malmstrom, and M. Johansson, "Biobased UV-curable coatings based on itaconic acid," *J. Coat. Technol. Res.*, vol. 14, no. 4, pp. 851–861, 2017, doi: 10.1007/s11998-017-9949-y.

[34] P. Borysiuk, M. Derda, R. Auriga, P. Boruszewski, and S. Monder, "Comparison of selected properties of varnish coatings curing with the use of UV and UV-LED approach," *Ann. Warsaw Univ. Life Sci. – SGGW For. Wood Technol.*, vol. 92, pp. 49–54, 2015.

[35] R. Patel, M. L. Chaudhary, Y. N. Patel, and K. Chaudhari, "Fire-Resistant Coatings: Advances in Flame-Retardant Technologies , Sustainable Approaches , and Industrial Implementation," *Polymers (Basel).*, vol. 17, pp. 1–50, 2025, doi: 10.3390/polym17131814.

[36] M. Weng, Y. Fu, and W. Xu, "Flame-Retardant Coating on Wood Surface by Natural Biomass Polyelectrolyte via a Layer-by-Layer Self-Assembly Approach," *Forests*, vol. 15, 2024, doi: 10.3390/ f15081362.

[37] S. Pellerin, F. Samyn, S. Duquesne, and V. Landry, "Preparation and Characterisation of UV-Curable Flame Retardant Wood Coating Containing a Phosphorus Acrylate Monomer," *Coatings*, vol. 12, 2022, doi: 10.3390/ coatings12121850.

[38] L. A. Lowden and T. R. Hull, "Flammability behaviour of wood and a review of the methods for its reduction," *Fire Sci. Rev.*, vol. 2, pp. 1–19, 2013, doi: 10.1186/2193-0414-2-4.

[39] X. Li *et al.*, "Current states and future challenges of multifunctional flame-retardant polyurethane coatings," *RSC Appl. Interfaces*, vol. 2, no. 6, pp. 1527–1536, 2025, doi: 10.1039/d5lf00215j.

[40] A. B. Cigil, Y. Samet, A. Özde, C. Hızal, A. Yılmaz, and O. Esenturk, "UV-Curable Polyurethane-Based, Halogen-Free,CaB 4 O 7 Nanoparticles Decorated , Flexible Flame-Retardant Films," *J. Inorg. Organomet. Polym. Mater.*, vol. 35, pp. 8678–8693, 2025, doi: 10.1007/s10904-025-03813-5.

[41] N. G. El Khashab, S. A. H. Albohy, H. A. El‐Wahab, and C. M. S. . Moustafa M. G. Fouda, "Preparation and characterization of novel flame‐retardant paint of substituted cyclodiphosph (V) azane sulfonomide and their Cu(II), Cd(II) metal complexes as new additives for exterior wood coating protection," *Sci. Rep.*, vol. 14, pp. 1–19, 2024,

doi: 10.1038/s41598-024-64065-w.

[42] R. S. Patil, J. Thomas, M. Patil, and J. John, “To Shed Light on the UV Curable Coating Technology:Current State of the Art and Perspectives,” *J. Compos. Sci.*, vol. 7, 2023, doi: 10.3390/jcs7120513.

[43] F. O. Nitbani, P. Jiwamurwa, P. Tjitda, B. A. Nurohmah, and H. E. Wogo, “Preparation of Fatty Acid and Monoglyceride from Vegetable Oil,” *J. Oleo Sci.*, vol. 295, no. 4, pp. 277–295, 2020, doi: 10.5650/jos.ess19168.

[44] A. M. Patil, V. V Gite, H. D. Jirimali, and R. N. Jagtap, “Fully Biobased Nanocomposites of Hyperbranched-Polyol and Hydroxyapatite in Coating Applications,” *J. Polym. Environ.*, no. 0123456789, 2020, doi: 10.1007/s10924-020-01903-8.

[45] S. U. Chambhare, G. P. Lokhande, and R. N. Jagtap, “Design and UV-curable behaviour of boron based reactive diluent for epoxy acrylate oligomer used for flame retardant wood coating,” *Des. Monomers Polym.*, vol. 20, no. 1, pp. 125–135, 2017, doi: 10.1080/15685551.2016.1231029.

[46] ASTM International, “Standard Test Method for Film Hardness by Pencil Test 1,” 2010. doi: 10.1520/D3363-05R11E02.

[47] ASTM International, “Standard Test Methods for Measuring Adhesion by Tape Test 1,” 2012. doi: 10.1520/D3359-09E02.

[48] ASTM International, “ASTM D635, Standard Test Method for Rate of Burning and/or Extent and Time of Burning of Plastics in a Horizontal Position,” West Conshohocken, PA.

[49] H. Park, B. Oh, and K. J. Jang, “Deep learning denoising enables rapid SEM imaging under charging conditions for FE SEM , CD SEM , and review SEM,” *Sci. Rep.*, vol. 16, pp. 1–9, 2026, doi: 10.1038/s41598-025-33273-3.

[50] D. Ezzat, M. Youssif, H. Elhaes, and M. El, “XRD and UV–Vis studies of cellulose acetate film blended with different concentrations of nano‑metal oxide,” *Opt. Quantum Electron.*, vol. 56, no. 5, pp. 1–21, 2024, doi: 10.1007/s11082-024-06480-x.